Published in final edited form as:
Methods Cell Biol. 2009 ; 93: 157–177. doi:10.1016/S0091-679X(08)93009-0.

Total Internal Reflection Fluorescence (TIRF) Microscopy of *Chlamydomonas* Flagella

Benjamin D. Engel[1], **Karl-Ferdinand Lechtreck**[2], **Tsuyoshi Sakai**[3], **Mitsuo Ikebe**[3], **George B. Witman**[2], and **Wallace F. Marshall**[1]

[1]Department of Biochemistry and Biophysics, University of California, San Francisco San Francisco, CA 94158

[2]Department of Cell Biology, University of Massachusetts Medical School Worcester, MA 01655

[3]Department of Physiology, University of Massachusetts Medical School Worcester, MA 01655

Abstract

The eukaryotic flagellum is host to a variety of dynamic behaviors, including flagellar beating, the motility of glycoproteins in the flagellar membrane, and intraflagellar transport (IFT), the bidirectional traffic of protein particles between the flagellar base and tip. IFT is of particular interest, as it plays integral roles in flagellar length control, cell signaling, development, and human disease. However, our ability to understand dynamic flagellar processes such as IFT is limited in large part by the fidelity with which we can image these behaviors in living cells. This chapter introduces the application of total internal reflection fluorescence (TIRF) microscopy to visualizing the flagella of *Chlamydomonas reinhardtii*. The advantages and challenges of TIRF are discussed in comparison to confocal and differential interference contrast (DIC) techniques. This chapter also reviews current IFT insights gleaned from TIRF microscopy of *Chlamydomonas* and provides an outlook on the future of the technique, with particular emphasis on combining TIRF with other emerging imaging technologies.

I. Introduction

Nearly every cell in the human body projects a primary cilium from its apical surface into the extracellular environment. Once thought to be a vestigial remnant from our days as single-celled organisms, the primary cilium is now appreciated both as a mechanosensory organelle and as a specialized compartment for signaling pathways such as Hedgehog and PDGFRαα (Huangfu *et al*., 2003; Schneider *et al*., 2005; Singla and Reiter, 2006). Meanwhile, ciliary defects have been implicated in a wide array of human disorders, from polycystic kidney disease to retinal degeneration and hydrocephalus (Pazour and Rosenbaum, 2002; Bisgrove and Yost, 2006; Lechtreck *et al*., 2008).

For over 40 years, the humble green alga *Chlamydomonas reinhardtii* has carried the banner of flagellar biology. *Chlamydomonas* possesses a wealth of flagellar mutants, which have greatly informed our understanding of these organelles. The cell's two flagella (identical to cilia in every way but their name) are readily purified for biochemical studies (King, 1995) and are amenable to numerous experimental perturbations, including regeneration after amputation (Rosenbaum *et al*., 1969; Lefebvre, 1995). However, one of this little alga's

Contact: name: Wallace Marshall mail: Box 2200, 600 16th St., San Francisco, CA, 94158, USA Wallace.Marshall@ucsf.edu tel: (415) 514-4304 fax: (415) 502-4315.

greatest contributions to flagellar biology was the discovery and characterization of intraflagellar transport (IFT).

IFT is indispensable for the assembly and maintenance of eukaryotic flagella. The only way for axonemal precursors to reach the site of flagellar assembly at the flagellar tip is to be carried there by large IFT particles, powered by the anterograde motor heterotrimeric kinesin-2. At the tip, IFT particles are remodeled and loaded with axonemal turnover products for their return trip to the cell body, driven by the retrograde motor cytoplasmic dynein-1b. The IFT machinery is highly evolutionarily conserved and many *Chlamydomonas* genes that encode IFT proteins are homologous to human disease genes (Pazour *et al.*, 2000).

IFT is a live-cell microscopy-defined phenomenon. Though IFT particles (originally dubbed "rafts") had been observed in electron micrographs for decades, their function was not understood until IFT was visualized by DIC microscopy (Kozminski *et al.*, 1993). Subsequent biochemisty studies have revealed much about the composition (Piperno and Mead, 1997; Cole *et al.*, 1998) of IFT particles, as well as their interactions with specific axonemal precursors (Qin *et al.*, 2004; Hou *et al.*, 2007). In addition, cryo-electron tomography studies have produced insights into the modular 3D architecture of IFT particles (Pigino *et al.*, 2007). However, since IFT is a description of the movement of proteins, live-cell microscopy remains an invaluable technique for understanding this important cellular behavior. In this paper, we briefly review the history of transmitted light and fluorescence microscopy in *Chlamydomonas* and then detail the promising new application of TIRF microscopy to studying IFT and other dynamic flagellar processes.

II. Rationale: A History of Flagellar Microscopy in *Chlamydomonas*

A. Phase Contrast and Dark Field: Early Insights into Flagellar Motilities

Each new advance in imaging technology has yielded fresh perspectives on the numerous dynamic processes of *Chlamydomonas* flagella. Phase contrast microscopy was central to many of the early descriptions of *Chlamydomonas* flagellar behaviors, including the kinetics of flagellar regeneration and shortening under a variety of conditions (Rosenbaum *et al.*, 1969). Decades later, these careful measurements still provide the foundation for investigations into flagellar length control. Phase contrast was also utilized to observe the dynamic bidirectional movements of polystyrene microspheres along the surface of the flagellar membrane (Bloodgood, 1977). This motility was later associated with the movements of flagellar glycoproteins and *Chlamydomonas* gliding motility, which occurs when the cell's flagella adhere to a solid surface (Bloodgood, 1995). Dark field microscopy, which provides enough contrast to visualize the dynamic instability of individual microtubules, was used to elegantly observe the rotation of the central pair microtubules in detergent-treated *Chlamydomonas* flagella (Kamiya, 1982). However, little was known about the traffic of proteins within eukaryotic flagella until researchers began examining *Chlamydomonas* with differential interference contrast (DIC) microscopy.

B. DIC: The Discovery and Initial Characterization of IFT

IFT was first described by video-enhanced DIC microscopy in 1993 (Kozminski *et al.*, 1993), and for the following decade, this was the only technique available for visualizing IFT in living *Chlamydomonas* cells. While the molecular identities of the IFT proteins were elucidated by biochemistry, these experiments were guided by DIC microscopy of temperature-sensitive mutants. Following identification of the *fla10* mutant as a "kinesin-like protein" (Walther *et al.*, 1994; later shown to be part of heterotrimeric kinesin-2 by Cole *et al.*, 1998), DIC microscopy of *fla10* at the restrictive temperature revealed that kinesin-2 was required for IFT (Kozminski *et al.*, 1995a). Two groups took advantage of this

observation to identify at least 15 IFT proteins that were depleted from *fla10* flagella at the restrictive temperature (Piperno and Mead, 1997; Cole *et al.*, 1998). Thus, microscopy steered the biochemical isolation of the IFT proteins, and throughout the subsequent years, DIC mutant analysis continued to shed light on the mechanisms of IFT. For instance, the loss of only retrograde trafficking events in *fla15*, *fla16*, and *fla17* mutants correlated with the specific depletion of IFT complex A proteins from flagella, implying that complex A is exclusively required for retrograde transport (Piperno *et al.*, 1998). While the wild-type speeds of anterograde and retrograde transport were reported with the initial description of IFT, detailed DIC kymograph analysis of speeds and frequencies enabled numerous *fla* mutants to be classified as defective in one or more stages of IFT: particle loading at the base, anterograde transport, particle turnaround at the tip, and retrograde transport (Iomini *et al.*, 2001). DIC kymograph analysis has also revealed that the frequency of IFT is relatively constant in shortening, lengthening, and steady-state flagella (Dentler, 2005).

Although DIC microscopy was invaluable for the discovery and initial characterization of IFT, the technique suffers from a few major limitations. The quality of IFT visualization is highly contingent on how flagella are oriented in relation to the axis of shear (parallel provides the greatest contrast). DIC quality also varies depending on how flagella are immobilized (certain paralyzed strains work better than others and mounting cells on agarose pads decreases resolution; Kozminski, 1995b). However, the greatest drawback of DIC is the inability to distinguish the traffic of specific proteins. Although combining DIC with temperature-sensitive mutants enabled the correlation of different IFT proteins with distinct IFT behaviors (Piperno *et al.*, 1998; Iomini *et al.*, 2001), these observations are indirect. In order to further tease apart the intricacies of IFT, it is necessary to examine the dynamics of specific IFT proteins and cargos through fluorescence microscopy.

C. Fluorescence: Algae Meet GFP

The first fluorescence imaging of IFT was achieved in *C. elegans* in 1999 (Orozco *et al.*, 1999). In the last decade, tremendous work has gone into characterizing IFT in worms and nearly 20 IFT proteins have now been tagged with green fluorescent protein (GFP) (Snow *et al.*, 2004; Blacque *et al.*, 2006; Mukhopadhyay *et al.*, 2007; Ou *et al.*, 2007). By quantifying IFT speeds in several mutants, these worm studies provided insights into the coordination of different IFT proteins and anterograde motors (Ou *et al.*, 2005). Efforts to visualize IFT with GFP in other organisms, including *Chlamydomonas* (Mueller *et al.*, 2005; Qin *et al.*, 2007) *Trypanosoma* (Absalon *et al.*, 2008) and mammalian cells (Follit *et al.*, 2006), lagged behind for several years but are currently all areas of active research. Due to its GC-codon bias, *Chlamydomonas* does not easily express many foreign proteins (Heitzer *et al.*, 2007). At the same time that the first fluorescent IFT proteins were being put into worms, *Chlamydomonas* received a codon-optimized EGFP that fortuitously eliminated a cryptic splice site from the original sequence (Fuhrmann *et al.*, 1999). Six years later, KAP (kinesin-associated protein, the non-motor subunit of heterotrimeric kinesin-2) became the first GFP-labeled IFT protein in *Chlamydomonas* (Fig. 2E; Mueller *et al.*, 2005). Since then, additional IFT proteins have been tagged, including IFT27 (Fig. 2D; Qin *et al.*, 2007), IFT20 (Fig. 2B, 2C and Fig. 4; Lechtreck *et al.*, 2009a), and BBS4 (Fig. 4; Lechtreck *et al.*, 2009a). The signaling protein CrPKD2 has also been labeled with GFP, revealing that ~10% of flagellar CrPKD2 undergoes anterograde transport, likely as an IFT cargo (Huang *et al.*, 2007).

While fluorescence imaging of IFT in *Chlamydomonas* has its share of hurdles (difficulties with protein expression, no homologous recombination, cells are autofluorescent and highly motile), there are significant advantages as well. At ~12μm, wild-type *Chlamydomonas* flagella are twice as long as *C. elegans* sensory cilia and most mammalian primary cilia, enabling a more detailed analysis of protein traffic. Furthermore, *Chlamydomonas* flagella

extend away from the cell body, which greatly enhances the signal-to-noise ratio by allowing the flagella to be imaged upon a dark background. In contrast, mammalian primary cilia must contend with the backdrop of a GFP-expressing cell. Finally, *Chlamydomonas* is endowed with a rich catalogue of flagellar mutants, such as the kinesin-2 mutant *fla10* (Huang *et al.*, 1977; Walther *et al.*, 1994), which can be mated to GFP-tagged strains to observe altered IFT dynamics.

D. TIRF Microscopy: A Perfect Match for *Chlamydomonas*

The imaging advantages of examining GFP-labeled flagellar proteins in *Chlamydomonas* become significantly pronounced with the addition of TIRF microscopy. While spinning disk confocal microscopy is superior to epifluorescence (less rapid GFP bleaching and better signal-to-noise by omitting out-of-focus light), TIRF provides even greater imaging fidelity at video rate speeds (compare Figs. 2B and 2C). Instead of passing the excitation laser through the sample like confocal microscopy, with TIRF the angle of incident light is increased until a critical angle is reached where all the light is reflected from the interface between the higher refractive index glass (n=1.518) and lower refractive index aqueous medium (n=1.33-1.38). Although no incident light penetrates the sample, it generates an electromagnetic field in the lower refractive index medium, known as the evanescent wave. This TIRF field has the same wavelength as the incident light and decays exponentially as it propagates from the interface, illuminating only the bottom few hundred nanometers of the sample (Axelrod, 2001).

Chlamydomonas is an ideal specimen for TIRF microscopy due to its natural gliding behavior. When *Chlamydomonas* encounters a solid substrate such as the coverglass, it tightly adheres both flagella to the glass, orienting them 180 degrees from each other (Bloodgood, 1977; 1995). Since the flagella are roughly 200nm thick, they fit perfectly within the evanescent field, while the large autofluorescent cell body is excluded from the field of illumination (Fig. 1A). Multiple through-the-objective TIRF systems are commercially available, each equipped with high NA objectives that are capable of producing the increased angles of incident illumination required for TIRF (for the images in Fig. 2, we used a Nikon TE2000-E inverted scope equipped with a 100x/1.49NA TIRF objective, the exceptionally useful Nikon Perfect Focus System, and a cooled Photometrics QuantEM:512SC EMCCD camera with quantitative gain).

By eliminating light pollution from the rest of the sample, TIRF achieves exceptional signal-to-noise, enabling the clear visualization of low abundance proteins, such as BBS4-GFP, that would otherwise be difficult to detect (Fig. 4). We utilized this improved image fidelity to assay the protein content of IFT particles in regenerating *Chlamydomonas* flagella. With TIRF, we managed to quantify not only the speed and frequency of IFT events, but also the GFP intensity of these trafficking IFT particles (Engel *et al.*, 2009). We found that the KAP-GFP and IFT27-GFP intensities of particles in short flagella were several times brighter than particles in long flagella, suggesting that particles in short flagella are assembled from more IFT proteins. We confirmed this disparity in protein content by counting the stepwise GFP bleaching events of particles in formaldehyde-fixed flagella exposed to TIRF illumination. Because TIRF has exceptional signal detection and slower photobleaching kinetics, many distinct GFP steps can be identified, especially when the bleach intensity plots are enhanced with an edge-preserving filter (Chung and Kennedy, 1991; Leake *et al.*, 2006). Thus, by simply applying TIRF techniques to existing GFP-labeled *Chlamydomonas* strains, we were able to revise the balance-point model of flagellar length control (proposed in Marshall *et al.*, 2001, 2005), concluding that IFT particle size scales inversely with flagellar length.

A clear advantage of fluorescence microscopy (and TIRF in particular) is the ability to follow the traffic of specific GFP-tagged flagellar proteins. While DIC primarily visualizes

large, processive anterograde and retrograde particles (Fig. 2A; Kozminski *et al.*, 1993; Iomini *et al.*, 2001; Dentler, 2005), TIRF microscopy of *Chlamydomonas* flagella has revealed different classes of IFT behavior. KAP-GFP, IFT27-GFP, and IFT20-GFP all have large anterograde particles that move with the same frequency and speed as the anterograde particles seen in DIC (Fig. 2A-E). However, while IFT27-GFP has processive retrograde transport similar to particles imaged by DIC (Fig. 2D), IFT20-GFP has slow, thick retrograde traces that frequently pause or change speeds (Figs. 2B and 2C). KAP-GFP, meanwhile, shows very few retrograde traces at all and has much higher background flagellar fluorescence than IFT27-GFP and IFT20-GFP, particularly toward the flagellar tip (Fig. 2E). Thus, the observation of only three GFP-labeled proteins has already begun to reveal several new intricacies of IFT. All three proteins likely travel out to the flagellar tip together at ~2um/s, in large processive anterograde particles that are clearly visible by DIC (Figs. 2F and 2G). At the tip, it is possible that some proteins, including the kinesin-2 anterograde motor and IFT20, which helps link kinesin-2 to IFT complex B, detach from these large particles. While the core of IFT complex B (including IFT27) undergoes processive retrograde transport in a protein complex large enough to be seen by DIC, IFT20 (perhaps bound to neighboring peripheral proteins such as IFT57) appears to undergo slower and less processive transport in complexes that may be too small for DIC visualization. Meanwhile, it is possible that many kinesin-2 proteins do not partake in retrograde transport at all, but rather remain diffuse in the flagellum. This observation potentially conflicts with the model that kinesin-2 is transported out of flagella on retrograde IFT particles powered by cytoplasmic dynein (Signor *et al.*, 1999). It should be noted that the divergent retrograde behaviors of IFT20-GFP and KAP-GFP could be the result of interference from the GFP tags. However, IFT20-GFP and KAP-GFP both fully rescue endogenous protein mutations and both have anterograde transport that is identical to IFT27-GFP and IFT observed by DIC, suggesting that the GFP-labeled proteins function normally. In addition, all three GFP-tagged proteins have reduced retrograde frequencies compared to frequencies that have been reported by DIC (Iomini *et al.*, 2001; Dentler, 2005). This may be due to detection limits of the TIRF technique, or it may present additional evidence that there are several different species of retrograde particles that cannot be distinguished by DIC. Of course, it is of great interest to label other IFT proteins with GFP to compile a complete description of which proteins share different IFT behaviors.

III. Materials and Methods: Technical Considerations of *Chlamydomonas* TIRF

A. Slide Preparation and Cell Immobilization

Preparing GFP-labeled *Chlamydomonas* cells for observation by TIRF microscopy is straightforward. After growing cells in liquid media, simply plate a small volume (~15μL) on untreated coverglass (we use #1.5). Though specially conditioned coverglass may also work, *Chlamydomonas* cells readily adhere to untreated glass. It is necessary to place a spacer between the slide and coverglass (we use a square ring of petroleum jelly) to prevent cells from being crushed. Focusing on the interface between the coverglass and the media should reveal numerous adherent cells whose flagella are perfectly positioned for TIRF microscopy.

While the unique gliding motility of *Chlamydomonas* cells makes TIRF imaging possible, it also poses one of the greatest obstacles to the technique. Although cells often remain in a stationary gliding position for up to a minute, which is ample time to analyze IFT, cells are quite mobile and will either glide out of the field of view or detach from the coverglass altogether. This is further complicated by the phototactic and photophobic behaviors of *Chlamydomonas*. The mere act of observing the cells with TIRF illumination is enough to

either encourage cells to flee the field of view or cluster tightly together on the coverglass, depending on the strain. Mounting cells on an agarose pad is an effective tool for immobilizing *Chlamydomonas* cells for DIC or confocal microscopy. However, agarose pads rarely immobilize cells in a gliding position. Instead, the autofluorescent cell bodies are pressed against the coverglass (and into the TIRF field), while the flagella do not evenly adhere to the glass. Coating the coverglass with poly-lysine has also proved problematic for immobilizing gliding cells. At 0.1 mg/mL, poly-lysine slightly decreases cell motility. At increased concentrations (up to 10 mg/mL), gliding motility nearly stops, but the tips of adherent flagella begin to curl up and cells deflagellate, leaving their flagella behind on the coverglass (Kozminski, 1995b). Additionally, because poly-lysine has a higher refractive index than aqueous media, it can interfere with the propagation of the evanescent wave and cause light scattering and increased background signal (George, 2008). When considering coverglass coatings, it is also important to ensure that the layers are thin so they will not occupy a significant portion of the TIRF field. It is possible that a more specific coating, such as antibodies to the flagellar membrane glycoprotein FMG1 (Bloodgood *et al.*, 1986), might prove more effective. However, even if we could completely immobilize the flagella to a substrate, *Chlamydomonas* may simply shed their flagella as seen with poly-lysine.

We have had greater success by crossing GFP strains to mutants with paralyzed flagella (such as the central-pair mutant *pf18*). While these cells tend to remain adhered to one spot for significantly longer time periods than wild-type cells, ultimately they too glide away or detach. There are additional *Chlamydomonas* mutants that may prove useful for immobilizing cells in the gliding position. *ptx* mutants are defective in phototaxis, and thus may not react to the excitation light (Horst and Witman, 1993). Concanavalin A has been reported to interfere with gliding motility in the *L-23 pf18* mutant (Bloodgood and Salomonsky, 1989). There are also a large number of *gli* mutants that were isolated by screening for gliding defects (Kozminski, 1995c), though the identities of these genes remain unknown, which complicates potential crosses to GFP strains. It is also important to note that mutant backgrounds may introduce unexpected variables (for example, *pf18* cells regenerate their flagella with slowed kinetics), and thus should always be compared to wild-type cells. Finally, gliding motility is reportedly inhibited by lowering the free calcium concentration with EGTA and adding 100mM NaCl (Kozminski *et al.*, 1993; Bloodgood, 1995). However, these conditions also induce flagellar resorption through unknown mechanisms (Lefebvre *et al.*, 1978), and consequently are less useful for observing flagella under steady-state length conditions. The immobilization of adherent *Chlamydomonas* cells during TIRF microscopy remains an unresolved issue, and until a solution is found, confocal and DIC microscopy will maintain an advantage for the prolonged observation of single cells.

B. The Angle of Incidence and Depth of the TIRF Field

The depth of the evanescent field varies greatly as a function of the excitation laser's angle of incidence. Greater angles create shallower fields (Mattheyes and Axelrod, 2006), so for most flagellar imaging applications, the incident angle should be reduced to near the critical angle to ensure the deepest possible TIRF field. By adjusting the angle of incidence very close to the critical angle, we have measured TIRF fields on our microscope that are 250nm-300nm deep (Engel *et al.*, 2009). Even though this is enough to image completely through *Chlamydomonas* flagella, it is very important to note that TIRF illumination is not constant, but rather falls off exponentially as a function of distance from the coverglass (Axelrod, 2001). This property of the evanescent field should always be considered when interpreting results. For example, when comparing IFT particles within a flagellum, it is impossible to distinguish whether differences in intensity are due to unequal protein content or different positions of the particles on the axoneme (Fig. 1B). However, it is legitimate to

compare the average intensity of IFT particles between different flagella (as shown in Engel *et al.*, 2009). The relationship between axoneme geometry and the TIRF field also increases the variability of GFP step sizes during quantitative photobleaching of fixed cells. GFP molecules that are further from the coverglass produce less intensity and are also less likely to bleach (Fig. 1B). Thus, although many GFP step sizes are similar, it is not uncommon to see a few smaller steps towards the end of the bleach. Since even slight variations in the incident angle significantly impact GFP intensity and the depth of the evanescent field, motorized control of the laser trajectory is quite useful, especially when trying to be consistent between imaging sessions. Other parameters, such as laser power and camera settings should also be kept constant when attempting to compare intensities between images. Many new EMCCD cameras are equipped with linear gain, which increases the reliability of comparing intensities between images. However, gain decreases as EMCCD cameras age (Ingley *et al.*, 2008), so imaging sessions should be performed as close together as possible.

C. GFP Labeling of *Chlamydomonas* Flagellar Proteins

Fluorescence detection is greatly increased if every copy of a specific flagellar protein is labeled with GFP. Furthermore, complete labeling enables quantification of protein abundance via intensity measurements and quantitative photobleaching (Engel *et al.*, 2009). However, since targeted gene deletion and homologous recombination are not simple feats in *Chlamydomonas*, the best candidates for GFP-labeling are IFT genes that already have identified *Chlamydomonas* mutations. These mutants can then be rescued with genes encoding GFP-tagged versions of the proteins. Rescuing IFT mutants provides the additional advantage of demonstrating that the exogenous GFP-labeled protein is functioning correctly. Moreover, when tagged proteins are expressed in the presence of the untagged endogenous protein, the latter may out-compete the former for interaction with a limited number of binding partners (Lechtreck *et al.*, 2009b). The existing GFP-tagged IFT20 and BBS4 strains are in null mutant backgrounds, where all endogenous flagellar protein has been replaced with the labeled version (Fig. 3, Lechtreck *et al.*, 2009a). KAP-GFP was expressed in the temperature-sensitive KAP mutant, *fla3* (Mueller *et al.*, 2005). However, at all temperatures, the flagellar KAP population is almost completely labeled with GFP (minute levels of the endogenous mutant protein may remain, see Fig. 3). IFT27-GFP, on the other hand, was expressed in wild-type cells. As a result, only half of the flagellar IFT27 protein is GFP-labeled, yielding a much weaker fluorescent signal (compare Fig. 2D with 2C and 2E; Qin *et al.*, 2007).

Two distinct cloning strategies have been successfully employed for GFP-labeling in *Chlamydomonas*: 1) Insertion of the tag sequence into an exon near the 3' end of the target gene (KAP-GFP) and 2) fusion of fluorescent proteins to the C-terminus of the target proteins (IFT27-GFP, CrPKD2-GFP, IFT20-GFP, IFT20-mCherry, BBS4-GFP). Proteins can be expressed either from vectors containing genomic sequences including the endogenous promoters (KAP-GFP, IFT27-GFP, CrPKD2-GFP) or from vectors using the *HSP70B/rbcS* or *FLA14* promoters, the latter of which was used to express cDNAs of *IFT20* and *BBS4*. Because the *FLA14* gene does not contain introns, its promoter efficiently expresses intronless cDNA. Furthermore, since *FLA14* encodes the flagellar dynein light chain LC8 (Pazour *et al.*, 1998), tagged flagellar proteins (such as IFT20-GFP) are expressed by the *FLA14* promoter at relatively wild-type levels and have equal flagellar abundance to endogenous protein in wild-type cells (Fig. 3).

Chlamydomonas cells can be transformed with linearized plasmids using the glass-bead method (Kindle, 1990) or electroporation (Shimogawara *et al.*, 1998). Screening transformants for rescue of a selectable phenotype enables thousands of transformants to be screened and strains expressing fusion proteins to be easily identified. IFT20-GFP, for

example, was expressed in an *ift20* deletion mutant, which is immotile due to the lack of flagella. Transformants were selected for restoration of motility, and expression of the GFP-fusion protein was then verified. If phenotypic selection of cells is not possible, cells expressing the fusion protein may be identified by fluorescence microscopy and western blotting. In our experience, FACS identification of GFP-expressing cells is difficult because the strong autofluorescence of the cell body masks GFP emission, but it may be possible to apply this approach to "white" *Chlamydomonas* mutants (McCarthy *et al.*, 2004).

IV. Discussion: Future Prospects for *Chlamydomonas* TIRF

A. Simultaneous Multi-Color TIRF

Simultaneously observing two or more proteins tagged with different color fluorophores holds great promise for understanding the co-localization of multiple IFT proteins and cargos as they transit through the flagellum. Considering that our initial observations appear to have revealed different classes of retrograde behaviors (Fig. 2), it will be of great interest to visualize which proteins traffic together.

In principle, there are few limitations to labeling numerous flagellar proteins with different fluorophores. Initially, *Chlamydomonas* IFT proteins had only been tagged with codon-optimized GFP because of concerns about protein expression. However, IFT20 fused to a synthetic mCherry sequence optimized for human codon bias was successfully expressed (Fig. 4; Lechtreck *et al.*, 2009a), opening the door to two-color experiments. IFT20-mCherry was observed to be less photostable and half as bright as IFT20-GFP. Initial observations of cells expressing both IFT20-mCherry and BBS4-GFP revealed that BBS4 is carried by only a subset of anterograde particles (Fig. 4). YFP and CFP variants of codon-optimized GFP have also been expressed in *Chlamydomonas* (Feldman, 2008), providing additional avenues for multi-color imaging.

Simultaneous multi-color TIRF presents several unique hurdles compared to single-channel imaging. In order to cleanly image two colors simultaneously, several specialized pieces of equipment are required, including a multiline laser launch, a multipass dichroic mirror that directs both excitation wavelengths to the sample, and an emission splitter (such as Photometrics Dual-View or Cairn OptoSplit) that separates each emission wavelength to opposite halves of a single camera or two different cameras. (The movie in Fig. 4 was acquired with an Olympus IX71 Inverted Microscope equipped with an Olympus 60x/1.4NA PlanApo objective, a Semrock FF498/581 multipass beam splitter with laser-line filters to clean the two colors of excitation light, a custom-built emission splitter system with a Semrock FF562-Di01 dichroic mirror and Semrock 525/50nm and 630/69nm emission filters that block both excitation wavelengths, and an Andor iXon DV860 back-illuminated EMCCD camera).

Most commercially available TIRF systems use a single fiber-optic cable to deliver multiple laser wavelengths to the sample. These systems can only introduce light at one incident angle and at one focus setting, which creates two complications for multi-color imaging. The first issue to consider is the effect of excitation color on laser focusing. Because different wavelengths of light are refracted at different angles when passing through the objective, they do not share the same focal point. Unless each laser is independently focused, the beam will be slightly less collimated, leading to increased light scattering and background signal (George, 2008). The second issue to consider is the effect of laser color on the depth of the evanescent field. The depth of field penetration depends on the refractive indices of the coverglass (n=1.518) and the aqueous medium (n=1.33-1.38), in addition to both the angle and wavelength of the incident illumination (Axelrod, 2001; George, 2008). Since the refractive indices of the imaging setup are relatively fixed, the angle of incidence must be

adjusted for different excitation wavelengths to maintain the same depth and intensity of TIRF illumination. Even with motorized control of laser trajectory, tuning the incident angle when switching between excitation colors introduces too great a lag for the simultaneous imaging of fast-moving IFT particles. While neither of these wavelength-related effects is severe, simultaneous multi-color TIRF would benefit from an imaging setup with separate light paths for each laser, each with its own independent angle and focus adjustments.

B. FRAP, Photoactivation, and Photoconversion

Several advanced photobleaching and photoactivation techniques can be combined with TIRF to shed light on additional aspects of IFT. Measuring the kinetics of FRAP (fluorescence recovery after photobleaching) may yield insights into how readily different IFT proteins in the flagella exchange with the cytoplasm. Tagging IFT proteins with photoactivatable or photoconvertable fluorophores would provide a reciprocal approach to this question. Photoactivation in the cytoplasm would facilitate the observation of protein exchange into the flagella. Because *Chlamydomonas* is biflagellate, photoactivating within one flagellum would also be highly informative. Protein exchange could be judged not only by loss of fluorescent IFT particles within the photoactivated flagellum, but also by the appearance of fluorescence in the dark flagellum. Finally, photoactivation and photoconversion would provide useful tools for understanding the dynamics of IFT turnaround at the flagellar tip. By only activating a small subset of the IFT particles in a flagellum, it would become clear whether particles immediately undergo retrograde transport when they reach the tip, and whether retrograde KAP (Fig. 2E) truly is diffuse or whether it undergoes an active transport mechanism that is undetectable in fully-labeled KAP-GFP flagella.

One potential obstacle to these promising experiments is the expression of photoactivatible and photoconvertible proteins in *Chlamydomonas.* The design of photoactivatible GFP (PA-GFP) should only require the straight-forward task of making a few simple base pair changes to the codon-optimized GFP sequence (following the scheme outlined by Patterson and Lippincott-Schwartz, 2002). The expression of more exotic fluorophores, such as the green-to-red photoconvertable proteins Kaede (Ando *et al.*, 2002), EosFP (Wiedenmann *et al.*, 2004), and Dendra2 (Labas *et al.*, 2002; Adam *et al.*, 2009), and the reversibly photoswitchable Dronpa (Habuchi *et al.*, 2005) may require codon optimization. However, it is possible that, like mCherry, these proteins will express without alterations to their sequence.

The greatest challenge to performing FRAP or photoactivation in TIRF will probably be the immobilization of *Chlamydomonas* cells. As previously discussed, even paralyzed strains glide out of the field of view or detach from the coverglass within minutes. It is likely that *Chlamydomonas* will have a strong photophobic response to the intense laser energy required for FRAP. Furthermore, the phototropin blue-light receptors localized in *Chlamydomonas* flagella (Huang *et al.*, 2004) will certainly be stimulated by the 405nm light used to activate PA-GFP, though the function of these photoreceptors is unknown. It is possible that a combination of the strategies discussed in section IIIA (such as *ptx* mutants and calcium depletion) will immobilize adherent cells long enough to facilitate these powerful protein tracking techniques. For some questions, such as protein exchange between the flagellar and cytoplasmic pools, confocal microscopy should suffice, allowing immobilization on agarose pads.

C. Applications Beyond IFT

TIRF should prove equally beneficial to imaging other *Chlamydomonas* flagellar proteins that are not continuously trafficked by IFT. This includes monitoring the dynamics of

membrane-bound signaling proteins, such as CrPKD2-GFP (Huang *et al.*, 2007) and tracking changes in flagellar membrane glycoprotein distribution (Bloodgood *et al.*, 1986). FRAP is not limited to studying the exchange of IFT particles, but can also be used to examine the turnover of membrane proteins and integrated axonemal proteins, such as dynein arms (Watanabe *et al.*, 2004). Based on the incorporation of HA-tubulin in quadraflagellates, it had been concluded that axonemal tubulin does not treadmill (Marshall *et al.*, 2001). However, this hypothesis could be tested more elegantly in live cells by either speckling axonemal tubulin with GFP (Waterman-Storer and Danuser, 2002) or by bleaching a fiducial mark on a fluorescent axoneme and monitoring this mark for movement. In another novel use of the technique, TIRF was recently combined with calcium-responsive dyes to measure transient spikes in flagellar calcium concentration. These transient calcium spikes rapidly increased in frequency prior to deflagellation (Wheeler *et al.*, 2008). Clearly, TIRF microscopy of *Chlamydomonas* flagella holds great promise for a range of applications beyond the study of IFT.

V. Summary

TIRF microscopy is a versatile new method for observing fluorescence in *Chlamydomonas* flagella. While there are still a few technical hurdles, such as protein expression and cell immobilization, TIRF provides greatly improved fidelity for imaging flagellar proteins in live cells. It has already provided some glimpses of new IFT behaviors (Fig. 2), but a wealth of untapped potential remains. Substantial inquiries into the mechanisms of IFT, as well as a full gamut of other flagellar biology questions, are waiting to be explored through additional protein labeling and the incorporation of multi-color, FRAP, and photoactivation techniques. Perhaps in the more distant future, it may even be possible to combine TIRF of *Chlamydomonas* flagella with super resolution technologies such as PALM/STORM (Betzig *et al.*, 2006; Rust *et al.*, 2006) and Structured Illumination (Gustafsson, 2000).

Supplementary Material

Refer to Web version on PubMed Central for supplementary material.

Acknowledgments

We thank Kurt Thorn and the Nikon Imaging Center at UC San Francisco for invaluable microscopy resources and assistance. We also thank Joshua Mueller, Mary Porter, Hongmin Qin, and Joel Rosenbaum for generously sharing GFP-labeled strains, as well as Kurt Thorn, Arthur Millius, Sarah Goodwin, Jennifer Blake and the Marshall Lab for helpful discussions and careful reading of the manuscript. This work was supported by the W. M. Keck Foundation Distinguished Young Scholars Program (W. F. Marshall), the Searle Scholar Program (W. F. Marshall), the Genentech Graduate Fellowship (B. D. Engel), National Institutes of Health Grant GM 030626 (G. B. Witman), and the Robert W. Booth Fund at the Greater Worcester Community Foundation (G. B. Witman).

References

Absalon S, Blisnick T, Kohl L, Toutirais G, Doré G, Julkowska D, Tavenet A, Bastin P. Intraflagellar transport and functional analysis of genes required for flagellum formation in trypanosomes. Mol. Biol. Cell. 2008; 19:929–944. [PubMed: 18094047]

Adam V, Nienhaus K, Bourgeois D, Nienhaus GU. Structural basis of enhanced photoconversion yield in GFP-like protein Dendra2. Biochemistry. 2009 [Apr 16, Epub ahead of print].

Ando R, Hama H, Yamamoto-Hino M, Mizuno H, Miyawaki A. An optical marker based on the UV-induced green-to-red photoconversion of a fluorescent protein. Proc. Natl. Acad. Sci. U.S.A. 2002; 99:12651–12656. [PubMed: 12271129]

Axelrod D. Total internal reflection fluorescence microscopy in cell biology. Traffic. 2001; 2:764–774. [PubMed: 11733042]

Bisgrove BW, Yost HJ. The roles of cilia in developmental disorders and disease. Development. 2006; 133:4131–4143. [PubMed: 17021045]

Blacque OE, Li C, Inglis PN, Esmail MA, Ou G, Mah AK, Baillie DL, Scholey JM, Leroux MR. The WD repeat-containing protein IFTA-1 is required for retrograde intraflagellar transport. Mol. Biol. Cell. 2006; 17:5053–5062. [PubMed: 17021254]

Betzig E, Patterson GH, Sougrat R, Lindwasser OW, Olenych S, Bonifacino JS, Davidson MW, Lippincott-Schwartz J, Hess HF. Imaging intracellular fluorescent proteins at nanometer resolution. Science. 2006; 313:1642–1645. [PubMed: 16902090]

Bloodgood RA. Motility occurring in association with the surface of the *Chlamydomonas* flagellum. J. Cell Biol. 1977; 75:983–989. [PubMed: 925091]

Bloodgood, RA. Flagellar surface motility: gliding and microsphere movements.. In: Dentler, W.; Witman, GB., editors. Methods in Cell Biology. Vol. 47. Elsevier Inc.; San Diego: 1995. p. 273-279.

Bloodgood RA, Salomonsky NL. Use of a novel *Chlamydomonas* mutant to demonstrate that flagellar glycoprotein movements are necessary for the expression of gliding motility. Cell Motil. Cytoskeleton. 1989; 13:1–8. [PubMed: 2731235]

Bloodgood RA, Woodward MP, Salomonsky NL. Redistribution and shedding of flagellar membrane glycoproteins visualized using an anti-carbohydrate monoclonal antibody and concanavalin A. J. Cell Biol. 1986; 102:1797–1812. [PubMed: 3009491]

Chung SH, Kennedy RA. Forward-backward non-linear filtering technique for extracting small biological signals from noise. J. Neurosci. Methods. 1991; 40:71–86. [PubMed: 1795554]

Cole DG, Diener DR, Himelblau AL, Beech PL, Fuster JC, Rosenbaum JL. *Chlamydomonas* kinesin-II-dependent intraflagellar transport (IFT): IFT particles contain proteins required for ciliary assembly in *Caenorhabditis elegans* sensory neurons. J. Cell Biol. 1998; 141:993–1008. [PubMed: 9585417]

Dentler W. Intraflagellar transport (IFT) during assembly and disassembly of *Chlamydomonas* flagella. J. Cell Biol. 2005; 170:649–659. [PubMed: 16103230]

Engel BD, Ludington WB, Marshall WF. Intraflagellar transport particle size scales inversely with flagellar length: revisiting the balance-point length control model. J. Cell Biol. 2009 [In review].

Feldman, JL. Ph.D. Thesis. University of California; San Francisco: 2008. Deconstructing Cell Architecture: Exploring centriole structure, function, and positioning in the green alga *Chlamydomonas reinhardtii*..

Follit JA, Tuft RA, Fogarty KE, Pazour GJ. The intraflagellar transport protein IFT20 is associated with the Golgi complex and is required for cilia assembly. Mol. Biol. Cell. 2006; 17:3781–3792. [PubMed: 16775004]

Fuhrmann M, Oertel W, Hegemann P. A synthetic gene coding for the green fluorescent protein (GFP) is a versatile reporter in *Chlamydomonas reinhardtii*. Plant J. 1999; 19:353–361. [PubMed: 10476082]

George NB. Overcoming optical challenges to live-cell TIRF microscopy. Biophotonics. 2008; 15:30–33.

Gustafsson MG. Surpassing the lateral resolution limit by a factor of two using structured illumination microscopy. J. Microsc. 2000; 198:82–87. [PubMed: 10810003]

Habuchi S, Ando R, Dedecker P, Verheijen W, Mizuno H, Miyawaki A, Hofkens J. Reversible single-molecule photoswitching in the GFP-like fluorescent protein Dronpa. Proc. Natl. Acad. Sci. U.S.A. 2005; 102:9511–9516. [PubMed: 15972810]

Heitzer M, Eckert A, Fuhrmann M, Griesbeck C. Influence of codon bias on the expression of foreign genes in microalgae. Adv. Exp. Med. Biol. 2007; 616:46–53. [PubMed: 18161490]

Horst CJ, Witman GB. ptx1, a nonphototactic mutant of *Chlamydomonas*, lacks control of flagellar dominance. J. Cell Biol. 1993; 120:733–741. [PubMed: 8425899]

Hou Y, Qin H, Follit JA, Pazour GJ, Rosenbaum JL, Witman GB. Functional analysis of an individual IFT protein: IFT46 is required for transport of outer dynein arms into flagella. J. Cell Biol. 2007; 176:653–665. [PubMed: 17312020]

Huang B, Rifkin MR, Luck DJ. Temperature-sensitive mutations affecting flagellar assembly and function in *Chlamydomonas reinhardtii*. J. Cell Biol. 1977; 72:67–85. [PubMed: 830657]

Huang K, Diener DR, Mitchell A, Pazour GJ, Witman GB, Rosenbaum JL. Function and dynamics of PKD2 in *Chlamydomonas reinhardtii* flagella. J. Cell Biol. 2007; 179:501–514. [PubMed: 17984324]

Huang K, Kunkel T, Beck CF. Localization of the blue-light receptor phototropin to the flagella of the green alga *Chlamydomonas reinhardtii*. Mol. Biol. Cell. 2004; 15:3605–3614. [PubMed: 15155806]

Huangfu D, Liu A, Rakeman AS, Murcia NS, Niswander L, Anderson KV. Hedgehog signalling in the mouse requires intraflagellar transport proteins. Nature. 2003; 426:83–87. [PubMed: 14603322]

Ingley R, Smith DR, Holland AD. Life testing of EMCCD gain characteristics. Nucl. Instrum. Methods Phys. Res., Sect. A. 2008; 600:460–465.

Iomini C, Babaev-Khaimov V, Sassaroli M, Piperno G. Protein particles in *Chlamydomonas* flagella undergo a transport cycle consisting of four phases. J. Cell Biol. 2001; 153:13–24. [PubMed: 11285270]

Kamiya R. Extrusion and rotation of the central-pair microtubules in detergent-treated *Chlamydomonas* flagella. Prog. Clin. Biol. Res. 1982; 80:169–173. [PubMed: 7100176]

Kindle KL. High-frequency nuclear transformation of *Chlamydomonas reinhardtii*. Proc. Natl. Acad. Sci. U.S.A. 1990; 87:1228–1232. [PubMed: 2105499]

King, SM. Large-scale isolation of *Chlamydomonas* flagella.. In: Dentler, W.; Witman, GB., editors. Methods in Cell Biology. Vol. 47. Elsevier Inc.; San Diego: 1995. p. 9-12.

Kozminski, KG. Ph.D. Thesis. Yale University; 1995c. Beat-independent flagellar motilities in *Chlamydomonas* and an analysis of the function of alpha-tubulin acetylation..

Kozminski, KG. High-resolution imaging of flagella.. In: Dentler, W.; Witman, GB., editors. Methods in Cell Biology. Vol. 47. Elsevier Inc.; San Diego: 1995b. p. 263-271.

Kozminski KG, Beech PL, Rosenbaum JL. The *Chlamydomonas* kinesin-like protein FLA10 is involved in motility associated with the flagellar membrane. J. Cell Biol. 1995a; 131:1517–1527. [PubMed: 8522608]

Kozminski KG, Johnson KA, Forscher P, Rosenbaum JL. A motility in the eukaryotic flagellum unrelated to flagellar beating. Proc. Natl. Acad. Sci. U.S.A. 1993; 90:5519–5523. [PubMed: 8516294]

Labas YA, Gurskaya NG, Yanushevich YG, Fradkov AF, Lukyanov KA, Lukyanov SA, Matz MV. Diversity and evolution of the green fluorescent protein family. Proc. Natl. Acad. Sci. U.S.A. 2002; 99:4256–4261. [PubMed: 11929996]

Leake MC, Chandler JH, Wadhams GH, Bai F, Berry RM, Armitage JP. Stoichiometry and turnover in single, functioning membrane protein complexes. Nature. 2006; 443:355–358. [PubMed: 16971952]

Lechtreck KF, Delmotte P, Robinson ML, Sanderson MJ, Witman GB. Mutations in Hydin impair ciliary motility in mice. J. Cell Biol. 2008; 180:633–643. [PubMed: 18250199]

Lechtreck, KF.; Johnson, EC.; Sakai, T.; Ikebe, M.; Witman, GB. The *Chlamydomonas* BBSome is transported by a subset of IFT particles and *bbs* mutants abnormally accumulate flagellar signaling proteins.. 2009a. [Submitted]

Lechtreck KF, Luro S, Awata J, Witman GB. HA-tagging of putative flagellar proteins in *Chlamydomonas reinhardtii* identifies a novel protein of intraflagellar transport complex B. Cell Motil. Cytoskeleton. 2009b [Apr 20, Epub ahead of print].

Lefebvre, PA. Flagellar amputation and regeneration in *Chlamydomonas*.. In: Dentler, W.; Witman, GB., editors. Methods in Cell Biology. Vol. 47. Elsevier Inc.; San Diego: 1995. p. 3-7.

Lefebvre PA, Nordstrom SA, Moulder JE, Rosenbaum JL. Flagellar elongation and shortening in *Chlamydomonas*. IV. Effects of flagellar detachment, regeneration, and resorption on the induction of flagellar protein synthesis. J. Cell Biol. 1978; 78:8–27. [PubMed: 149796]

Marshall WF, Rosenbaum JL. Intraflagellar transport balances continuous turnover of outer doublet microtubules: implications for flagellar length control. J. Cell Biol. 2001; 155:405–414. [PubMed: 11684707]

Marshall WF, Qin H, Rodrigo Brenni M, Rosenbaum JL. Flagellar length control system: testing a simple model based on intraflagellar transport and turnover. Mol. Biol. Cell. 2005; 16:270–278. [PubMed: 15496456]

Mattheyses AL, Axelrod D. Direct measurement of the evanescent field profile produced by objective-based total internal reflection fluorescence. J. Biomed. Opt. 2006; 11:014006. [PubMed: 16526883]

McCarthy SS, Kobayashi MC, Niyogi KK. White mutants of Chlamydomonas reinhardtii are defective in phytoene synthase. Genetics. 2004; 168:1249–57. [PubMed: 15579683]

Mueller J, Perrone CA, Bower R, Cole DG, Porter ME. The FLA3 KAP subunit is required for localization of kinesin-2 to the site of flagellar assembly and processive anterograde intraflagellar transport. Mol. Biol. Cell. 2005; 16:1341–1354. [PubMed: 15616187]

Mukhopadhyay S, Lu Y, Qin H, Lanjuin A, Shaham S, Sengupta P. Distinct IFT mechanisms contribute to the generation of ciliary structural diversity in *C. elegans*. EMBO J. 2007; 26:2966–2980. [PubMed: 17510633]

Orozco JT, Wedaman KP, Signor D, Brown H, Rose L, Scholey JM. Movement of motor and cargo along cilia. Nature. 1999; 398:674. [PubMed: 10227290]

Ou G, Blacque OE, Snow JJ, Leroux MR, Scholey JM. Functional coordination of intraflagellar transport motors. Nature. 2005; 436:583–587. [PubMed: 16049494]

Patterson GH, Lippincott-Schwartz J. A photoactivatable GFP for selective photolabeling of proteins and cells. Science. 2002; 297:1873–1877. [PubMed: 12228718]

Pazour GJ, Dickert BL, Vucica Y, Seeley ES, Rosenbaum JL, Witman GB, Cole DG. *Chlamydomonas* IFT88 and its mouse homologue, polycystic kidney disease gene tg737, are required for assembly of cilia and flagella. J. Cell Biol. 2000; 151:709–718. [PubMed: 11062270]

Pazour GJ, Rosenbaum JL. Intraflagellar transport and cilia-dependent diseases. Trends Cell Biol. 2002; 12:551–555. [PubMed: 12495842]

Pigino G, Geimer S, Lanzavecchia S, Paccagnini E, Cantele F, Rosenbaum JL, Lupetti P. Electron tomographic analysis of intraflagellar transport complexes in situ. Mol. Biol. Cell. 2007; 18(suppl) abstract 272.

Piperno G, Mead K. Transport of a novel complex in the cytoplasmic matrix of *Chlamydomonas* flagella. Proc. Natl. Acad. Sci. U.S.A. 1997; 94:4457–4462. [PubMed: 9114011]

Piperno G, Siuda E, Henderson S, Segil M, Vaananen H, Sassaroli M. Distinct mutants of retrograde intraflagellar transport (IFT) share similar morphological and molecular defects. J. Cell Biol. 1998; 143:1591–1601. [PubMed: 9852153]

Qin H, Diener DR, Geimer S, Cole DG, Rosenbaum JL. Intraflagellar transport (IFT) cargo: IFT transports flagellar precursors to the tip and turnover products to the cell body. J. Cell Biol. 2004; 164:255–266. [PubMed: 14718520]

Qin H, Wang Z, Diener D, Rosenbaum JL. Intraflagellar transport protein 27 is a small G protein involved in cell-cycle control. Curr. Biol. 2007; 17:193–202. [PubMed: 17276912]

Rosenbaum JL, Moulder JE, Ringo DL. Flagellar elongation and shortening in *Chlamydomonas*. The use of cycloheximide and colchicine to study the synthesis and assembly of flagellar proteins. J. Cell Biol. 1969; 41:600–619. [PubMed: 5783876]

Rust MJ, Bates M, Zhuang X. Sub-diffraction-limit imaging by stochastic optical reconstruction microscopy (STORM). Nat. Methods. 2006; 3:793–795. [PubMed: 16896339]

Schneider L, Clement CA, Teilmann SC, Pazour GJ, Hoffmann EK, Satir P, Christensen ST. PDGFRalphaalpha signaling is regulated through the primary cilium in fibroblasts. Curr Biol. 2005; 15:1861–1866. [PubMed: 16243034]

Shimogawara K, Fujiwara S, Grossman A, Usuda H. High-efficiency transformation of *Chlamydomonas reinhardtii* by electroporation. Genetics. 1998; 148:1821–1828. [PubMed: 9560396]

Signor D, Wedaman KP, Orozco JT, Dwyer ND, Bargmann CI, Rose LS, Scholey JM. Role of a class DHC1b dynein in retrograde transport of IFT motors and IFT raft particles along cilia, but not dendrites, in chemosensory neurons of living Caenorhabditis elegans. J. Cell Biol. 1999; 147:519–530. [PubMed: 10545497]

Singla V, Reiter JF. The primary cilium as the cell's antenna: signaling at a sensory organelle. Science. 2006; 313:629–633. [PubMed: 16888132]

Snow JJ, Ou G, Gunnarson AL, Walker MR, Zhou HM, Brust-Mascher I, Scholey JM. Two anterograde intraflagellar transport motors cooperate to build sensory cilia on C. elegans neurons. Nat. Cell Biol. 2004; 6:1109–1113. [PubMed: 15489852]

Walther Z, Vashishtha M, Hall JL. The *Chlamydomonas* FLA10 gene encodes a novel kinesin-homologous protein. J. Cell Biol. 1994; 126:175–188. [PubMed: 8027176]

Watanabe Y, Hayashi M, Yagi T, Kamiya R. Turnover of actin in *Chlamydomonas* flagella detected by fluorescence recovery after photobleaching (FRAP). Cell Struct. Funct. 2004; 29:67–72. [PubMed: 15528838]

Waterman-Storer CM, Danuser G. New directions for fluorescent speckle microscopy. Curr. Biol. 2002; 12:R633–640. [PubMed: 12372272]

Wheeler GL, Joint I, Brownlee C. Rapid spatiotemporal patterning of cytosolic Ca2+ underlies flagellar excision in *Chlamydomonas reinhardtii*. Plant J. 2008; 53:401–413. [PubMed: 18086284]

Wiedenmann J, Ivanchenko S, Oswald F, Schmitt F, Röcker C, Salih A, Spindler KD, Nienhaus GU. EosFP, a fluorescent marker protein with UV-inducible green-to-red fluorescence conversion. Proc. Natl. Acad. Sci. U.S.A. 2004; 101:15905–15910. [PubMed: 15505211]

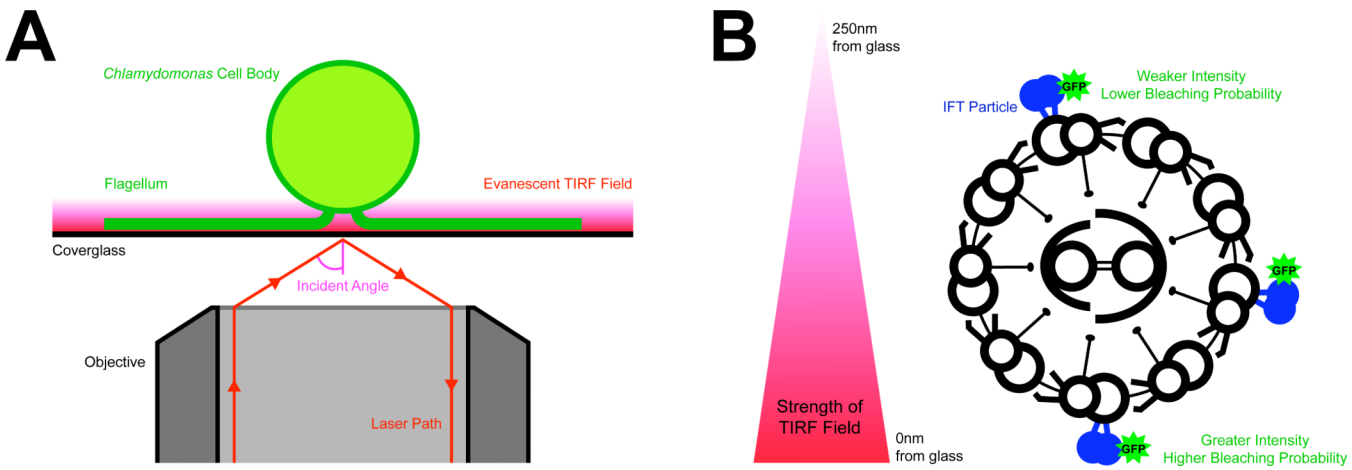

Figure 1. Chlamy TIRF Imaging Setup and the Effect of Axoneme Geometry on GFP Fluorescence

(A) Imaging of *Chlamydomonas* via through-the-objective TIRF. Excitation light comes out of the objective at an incident angle that is greater than the critical angle. The light is totally internally reflected, creating an evanescent field on the other side of the interface. Both flagella adhere to the coverglass and are readily imaged, while the cell body remains outside of the TIRF field. (B) Due to the ~200nm diameter of the axoneme, GFP molecules near the glass interface will be brighter and more likely to photobleach, while GFP proteins on the far side of the axoneme will produce a weaker signal, but are also less likely to bleach. This effect of the flagellar geometry should be considered during both live-cell imaging and fixed-cell quantitative photobleaching experiments.

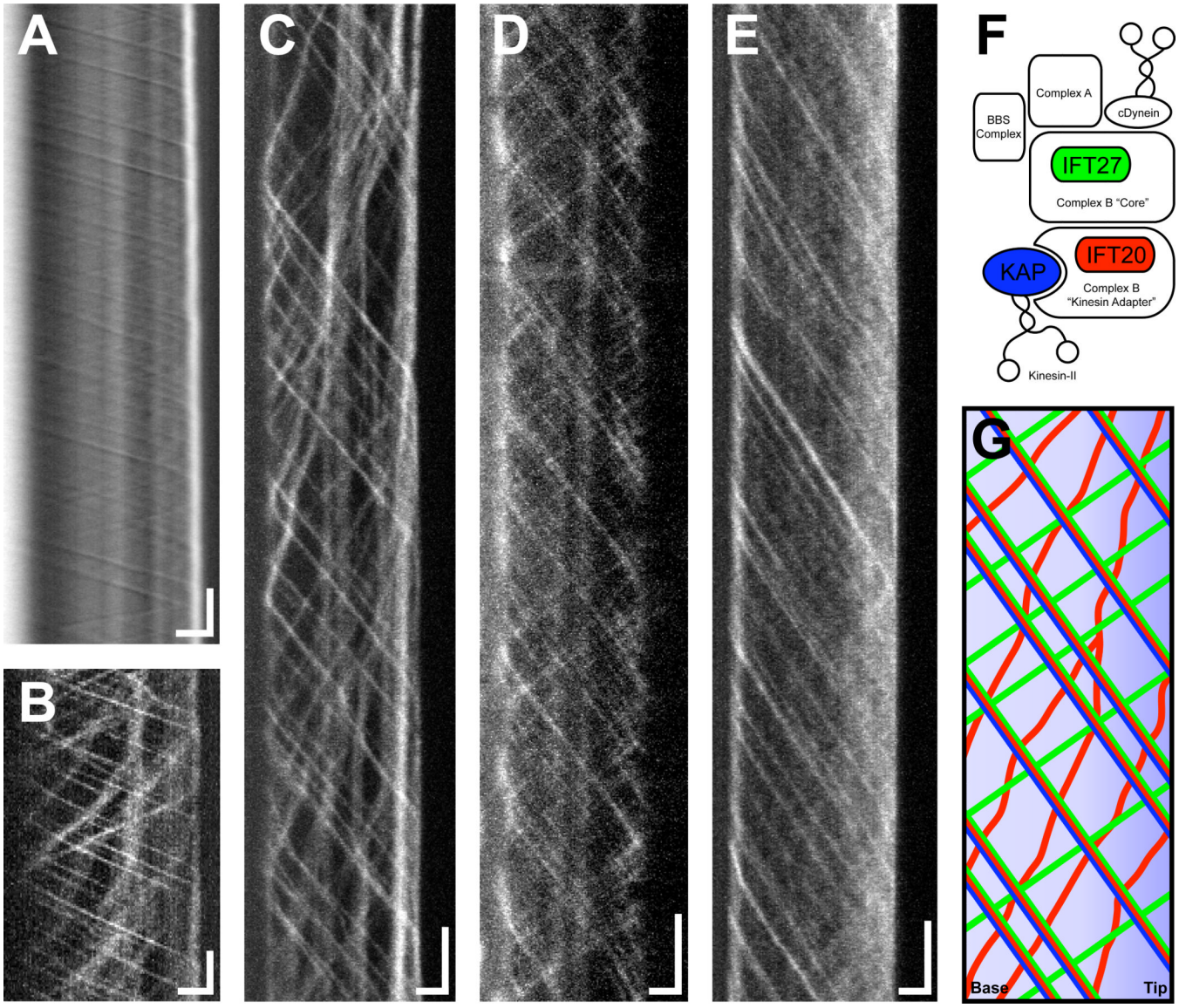

Figure 2. Comparison of DIC, Spinning Disk Confocal, and TIRF Microscopy and Summary of Current IFT Observations via TIRF

For all kymographs, the X-axis represents distance (base of flagellum on the left, tip on the right), while the Y-axis is time. Vertical scale bars: 2 sec; horizontal scale bars: 2 μm. (A) DIC kymograph of KAP-GFP *fla3*. Anterograde and retrograde traces are processive. Acquired at intermediate resolution with an .85NA dry condenser. For higher quality DIC kymographs of IFT (taken with 1.4NA oil condensers), see Iomini *et al.*, 2001 and Dentler, 2005. (B) Spinning disk kymograph of IFT20-GFP Δ*ift20*. Compare fidelity with the TIRF kymograph of IFT20-GFP Δ*ift20* in (C). Anterograde is processive, but retrograde has broad, slow traces that pause and change speed. (D) TIRF kymograph of IFT27-GFP in a wild-type background. Anterograde and retrograde traces are processive, similar to DIC. (E) TIRF kymograph of KAP-GFP *fla3*. Anterograde is processive but there are very few retrograde traces and the flagellar background is higher than IFT20-GFP or IFT27-GFP, especially towards the flagellar tip. Compare to the processive retrograde in the DIC kymograph in part A. (F) A hypothetical anterograde particle. The three GFP-labeled IFT

proteins are color-coded to match part G. (G) An illustrated kymograph that summarizes the behaviors of all three proteins seen in parts C, D, and E.

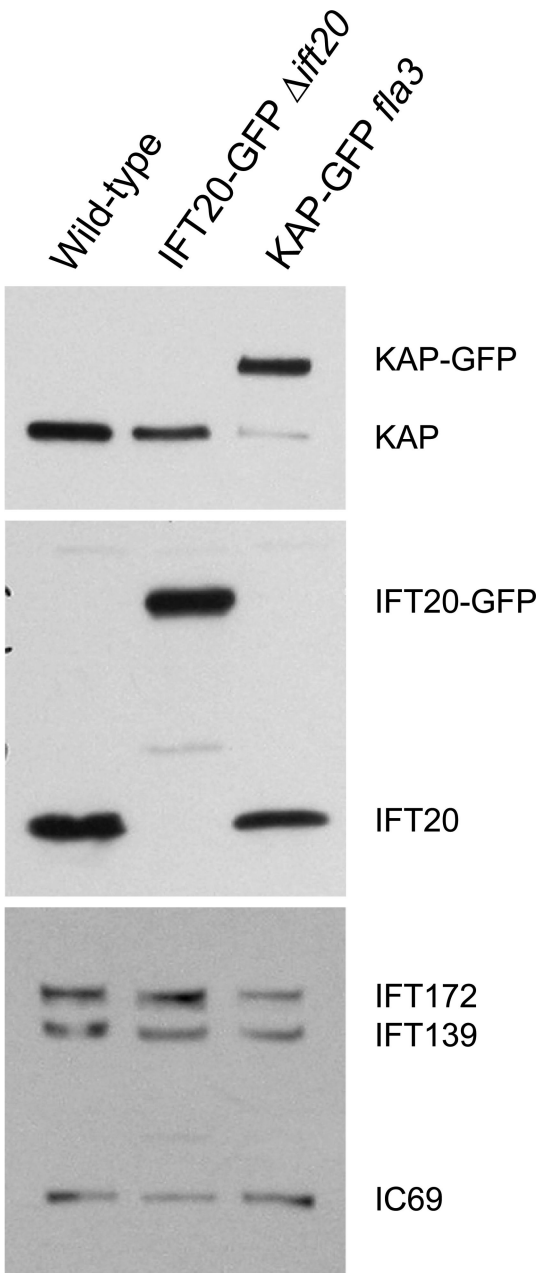

Figure 3. Protein Abundance in the Flagella of Wild-type and GFP-tagged Strains

Top panel: KAP-GFP *fla3* flagella almost exclusively contain KAP-GFP protein (though a small amount of endogenous protein remains). KAP-GFP levels are similar to endogenous KAP levels in wild-type and IFT20-GFP flagella. Middle panel: IFT20-GFP flagella only contain exogenous protein because the fusion protein was expressed in a null *ift20* background. IFT20-GFP levels are similar to endogenous IFT20 levels in wild-type and KAP-GFP flagella. Bottom panel: the expression of exogenous KAP-GFP and IFT20-GFP does not interfere with the flagellar levels of IFT172 (part of IFT complex B), IFT139 (part of IFT complex A), or IC69 (an intermediate chain of axonemal outer arm dynein). The top panel was probed with anti-KAP, the middle panel was probed with anti-IFT20, and the bottom panel was probed with anti-IFT172, anti-IFT139 and anti-IC69 antibodies.

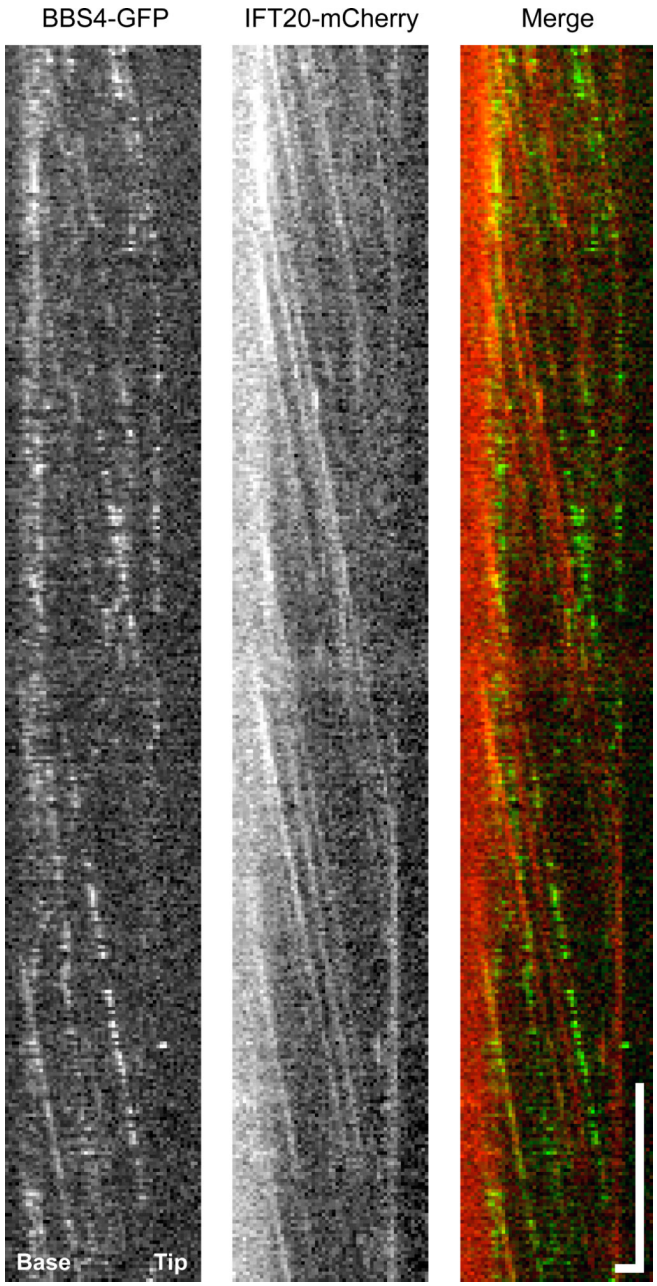

Figure 4. Simultaneous Two-Color TIRF of IFT20-mCherry and BBS4-GFP

For all kymographs, the X-axis represents distance (base of flagellum on the left, tip on the right), while the Y-axis is time. Vertical scale bar: 2 sec; horizontal scale bar: 2 μm. BBS4-GFP is much lower in abundance than IFT20-mCherry, and is only localized to a subset of the IFT20-mCherry particles. In the merged image, BBS4-GFP is green and IFT20-mCherry is red. Please see the color version of this kymograph online.